CALPHAD: Computer Coupling of Phase Diagrams and Thermochemistry 90 (2025) 102855

Contents lists available at ScienceDirect

Calphad

journal homepage: www.elsevier.com/locate/calphad

Experimental study and thermodynamic assessment of the $MgSO_4$-$CaSO_4$ system

Amedeo Morsa [a,*], Elena Yazhenskikh [a], Mirko Ziegner [a], Egbert Wessel [a], Rhys Dominic Jacob [a], Michael Müller [a], Dmitry Sergeev [a,b]

[a] Forschungszentrum Jülich GmbH, Institute of Energy Materials and Devices, Structure and Function of Materials (IMD-1), Jülich, D-52425, Germany
[b] NETZSCH-Gerätebau GmbH, Selb, D-95100, Germany

ARTICLE INFO

Keywords:
Phase change materials
Sulphates
Phase equilibria
Phase transition enthalpy
Database development

ABSTRACT

This work presents a comprehensive experimental investigation into the thermal properties of the binary system $MgSO_4$-$CaSO_4$, alongside thermodynamic modelling of its thermodynamic properties, with a focus on enhancing its application in thermal energy storage. The phase diagram and thermodynamic properties of the pure sulphates and intermediate compounds were determined using Differential Thermal Analysis (DTA) and Differential Scanning Calorimetry (DSC). The DSC results led to the refinement of the enthalpy values for phase transitions of $MgSO_4$, with updated values of 14.6 kJ/mol and 43.4 kJ/mol for the solid-solid and solid-liquid transitions, respectively. High-Temperature X-ray Diffraction (HTXRD) was employed to study the intermediate compounds, leading to the identification of $CaMg_2(SO_4)_3$. For the first time, the melting temperature and the enthalpy of fusion for this compound were experimentally determined, yielding a value of 145.5 kJ/mol at 1213 ± 5 °C. A novel phase with the composition $CaMg(SO_4)_2$ was identified using DTA, HTXRD, and Scanning Electron Microscopy (SEM). This phase exhibits a melting temperature of 1309 ± 5 °C, as determined by DTA, and demonstrates thermal stability within a high-temperature range of 1020–1308 °C. These experimental data were used to update the thermodynamic database for the system $MgSO_4$-$CaSO_4$ for more accurate thermochemical calculations and predictions.

1. Introduction

Magnesium sulphate ($MgSO_4$) and calcium sulphate ($CaSO_4$) are critical compounds in various industrial processes due to their dual roles in both facilitating and mitigating corrosion, as well as their emerging applications in energy storage technologies [1]. These sulphates are commonly found as by-products in systems where alkali and alkaline earth metals interact with sulphur-containing environments, leading to the formation of corrosive deposits. Such deposits can cause significant material degradation, particularly in high-temperature industrial settings, such as gas turbines, metallurgical processes, and cement production [2,3]. The aggressive nature of these sulphate melts necessitates a thorough understanding of their thermochemical properties to prevent material failure and extend the lifespan of industrial components. Understanding the thermal behaviour of sulphates in the $MgSO_4$-$CaSO_4$ system is crucial for addressing seawater-induced sulphur poisoning in Solid Oxide Electrolysis Cells (SOECs), as it directly influences the development of strategies to mitigate material degradation and enhance cell longevity in sulphur-rich environments [4,5].

Beyond their role in corrosion, sulphates have attracted interest in the field of thermal energy storage due to their potential as phase change materials (PCMs) [6]. The identification and characterisation of high-temperature PCMs are critical for advancing thermal energy storage technologies, which are essential for applications ranging from industrial processes to renewable energy systems. In the pursuit of identifying PCMs candidates, extensive research has been undertaken, both to identify suitable materials and to enhance system design and application [7,8]. Within the realm of high-temperature molten salt PCMs, the majority of research has focused on chloride, nitrate and carbonate mixtures [9–11]. While these materials have demonstrated considerable potential, issues related to corrosion and thermal stability have necessitated the exploration of alternative materials, such as sulphates. Given the limited thermodynamic data available in the literature, there is an urgent need to update thermodynamic databases based

* Corresponding author.
E-mail address: a.morsa@fz-juelich.de (A. Morsa).

https://doi.org/10.1016/j.calphad.2025.102855
Received 8 April 2025; Received in revised form 24 June 2025; Accepted 27 June 2025
Available online 30 June 2025

on new experimental findings. The integration of experimental research with the development of a comprehensive database will enable more accurate predictions of thermodynamic properties across various systems, ultimately advancing the field of PCMs. Several studies have been conducted on nitrates, chlorides, and sulphates to establish a robust database pertinent to high-temperature thermal energy storage [12–15]. The present study contributes to this ongoing effort by providing new data on sulphate-containing systems.

Among potential PCM candidates, $MgSO_4$ and $CaSO_4$ have attracted significant interest due to their favourable thermal properties and abundance. The relatively high melting points of $MgSO_4$ and $CaSO_4$ make them promising candidates for high-temperature energy storage applications, offering advantages in terms of reducing costs associated with containment and energy storage equipment [16]. Sulphates meet the thermodynamic, kinetic and economic criteria necessary for use as PCMs [17,18], such as high specific heat capacity, heat of fusion, and density, which are essential for minimizing the volume of heat storage units. However, they often fail to meet the chemical criteria due to their tendency to decompose at elevated temperatures and their corrosive nature, which pose challenges to their practical applications.

This study focuses on a detailed investigation of the phase behaviour of the $MgSO_4$-$CaSO_4$ system, with the objective of expanding the experimental data available. The experimental challenges associated with studying sulphates necessitate robust and innovative experimental techniques. This work employs advanced thermal analysis methods to accurately characterise the phase behaviour of $MgSO_4$ and $CaSO_4$, thereby providing a comprehensive dataset of thermodynamic properties.

The binary system $MgSO_4$-$CaSO_4$ was experimentally investigated only by Rowe et al. [19]. Ramsdell [20] and Mukimov et al. [21] assumed the phase diagram to be a simple binary eutectic system containing no intermediate compounds. Rowe et al. [19] reported instead the presence of an intermediate compound $CaSO_4 \cdot 3MgSO_4$ which melts congruently at 1201 ± 4 °C. The phase diagram was assumed to be a simple eutectic system with two eutectics at 13.5 mol% (unknown temperature) and 52 mol% of $CaSO_4$ (at 1116 °C). The liquidus temperatures were determined by sealed tube quenching experiments, the sub-solidus reactions were investigated by long-time annealing at temperatures below the decomposition temperatures. Calculated phase diagrams of this system [15,22] are in good agreement with the experimental values of Rowe et al. [19]. Du [22] modelled the congruent-melting compound $CaMg_3(SO_4)_4$. The optimised eutectic points were calculated at 1069 °C and 6.4 mol% and 1116 °C and 52 mol % $CaSO_4$, respectively. Yazhenskikh et al. [15] reported the calculated eutectic between $CaSO_4$ and $CaMg_3(SO_4)_4$ at 1117 °C with the composition of 53.0 mol% of $CaSO_4$, and the eutectic between $MgSO_4$ and $CaMg_3(SO_4)_4$ at 1071 °C and 5.5 mol% of $CaSO_4$.

The present study confirms, through new experimental evidence, the existence of the intermediate compound, $CaMg_2(SO_4)_3$, previously reported in Ref. [23]. Detailed characterisation of $CaMg_2(SO_4)_3$, including phase transition temperature, structural information, heat capacity and transition enthalpy, is provided in this work, necessitating a revision of the phase diagram and an update to the thermodynamic database. In addition to the intermediate compound with a 2:1 stoichiometric ratio, a 1:1 compound, stable within a restricted temperature range, was introduced into the assessment based on experimental findings, prompting further modifications to the phase equilibria. These findings result in significant updates to the $MgSO_4$-$CaSO_4$ phase diagram, underscoring the complexity of interactions in this system and providing new insights into the thermochemical behaviour of sulphate mixtures.

In this work, the Gibbs energy of all phases, including stoichiometric compounds and liquid solution in the $MgSO_4$-$CaSO_4$ system, has been reassessed based on the available and newly acquired data and included in the PCM database [15,24]. Thermodynamic data of pure $MgSO_4$ were assessed based on Differential Scanning Calorimetry (DSC) investigation of this work, while the data for pure $CaSO_4$ were re-assessed based on this and prior experimental research [25]. The Gibbs energy of $CaMg_2(SO_4)_3$ compound was modelled by using the heat capacity data measured in this work. The Gibbs energy of $CaMg(SO_4)_2$ compound was modelled using the Neumann-Kopp rule and subsequently optimised to accurately represent its thermal stability and phase equilibria. The liquid phase was described using the modified associate species model to keep consistency with the previous dataset [15].

Therefore, this research provides new experimental data for pure compounds and various sulphate mixtures across the full composition range of the $MgSO_4$-$CaSO_4$ system. It also delivers reassessed thermodynamic properties that enhance the existing database [15], by integrating novel findings that correct previous discrepancies and expand the understanding of phase stability and thermodynamic behaviour. The inclusion of these updated properties into the current database aims to support the accurate prediction of thermodynamic properties in related systems, advancing the development and optimisation of high-temperature phase change materials.

2. Experimental

2.1. Samples

The pure compounds $MgSO_4$ (VWR Chemicals, anhydrous ≥99 %, metal basis) and $CaSO_4$ (Alfa Aesar, anhydrous 99,993 %) were used for the preparation of the mixtures. Additionally, the powders were dried at 150 °C in a vacuum furnace for 24 h to remove the moisture prior to use. All manipulations with the samples were carried out in a glove box under dry argon atmosphere. The mixtures were prepared directly into crucibles according to the mass fraction with an amount of 50–100 mg, by sequentially adding the powdered components one on top of the other. The determination of the melting temperature of the pure compounds and mixtures under study is hampered by decomposition of the sulphates into oxides before reaching their melting temperatures [19,26–28]. The total mass loss attributed to this reaction amounted to 66.90 % and 60.85 % for $MgSO_4$ and $CaSO_4$ respectively, observed above 1000 °C and 1200 °C in open alumina crucibles from preliminary thermogravimetry tests. It is justifiable to infer that the residual 33.10 % and 39.15 % of the mass represent MgO and CaO respectively, which is in good agreement with the molar fraction of MgO in $MgSO_4$ (33.48 %) and CaO in $CaSO_4$ (41.19 %). Therefore, the measurements were conducted in sealed platinum crucibles in order to avoid mass loss due to the decomposition reaction and to achieve equilibrium conditions within the system.

2.2. Instruments

2.2.1. Differential Thermal Analysis and Thermal Gravimetry (DTA/TG)

DTA measurements were performed using a STA 449 C Jupiter (Netzsch) with a silicon carbide oven (RT-1600 °C) and a perpendicular sample holder with type S thermocouple (Pt/(Pt10Rh)). The temperature calibration was conducted using the structure and phase transitions temperatures of C_6H_5COOH (122.5 °C), $RbNO_3$ (164.2 °C), $KClO_4$ (300.8 °C), Ag_2SO_4 (462.2 °C), CsCl (470.0 °C), K_2CrO_4 (668.0 °C), $BaCO_3$ (808.0 °C), K_2SO_4 (1069.0 °C), CaF_2 (1418.0 °C), in sealed platinum tubes placed in alumina DTA crucibles. The resulting accuracy of transition temperature measurements is ±5 °C. The experiments were carried out with a heating rate of 5 K/min and three cycles of heating and cooling under an Ar atmosphere with a gas flow rate of 20 ml/min. All raw experimental data were evaluated with Proteus Analysis software from Netzsch. The results showed good reproducibility from the second cycle indicating a good equilibration of the samples. In this work, the phase transformation temperature was defined from the heating cycle and more specifically, the eutectic temperature was taken as the onset temperature, and the maximum peak temperature of further transformations was taken as the liquidus temperature or solid-solid transformation temperature. Due to the decomposition of sulphates,

the experimental melting temperatures of pure sulphate compounds may represent a minimum, because of the potential formation of MO (with M = Mg or Ca), which would reduce the liquidus temperature as the system becomes binary (MO-MSO_4). In order to prevent mass loss due to decomposition of sulphates, sealed crucibles were used for analysis. The crucible was closed by folding the upper end after filling the sample (50–100 mg) under dry argon in a glove box and then welded outside the glove box with a hydrogen/oxygen flame.

2.2.2. Differential Scanning Calorimetry (DSC)

Two different differential scanning calorimeters were used for the determination of thermodynamic properties. A differential scanning calorimeter DSC 404 Pegasus (Netzsch) with a Pt-Rh oven (RT-1600 °C) and type S thermocouple (Pt/(Pt10Rh)) was used to determine the heat capacity of selected compositions at temperatures below their decomposition points. The temperature calibration was performed with the pure compounds C_6H_5COOH (122.5 °C), $RbNO_3$ (164.2 °C), $KClO_4$ (300.8 °C), Ag_2SO_4 (462.2 °C), CsCl (470.0 °C), K_2CrO_4 (668.0 °C), $BaCO_3$ (808.0 °C), K_2SO_4 (1069 °C), CaF_2 (1418 °C). The average temperature deviation was ±2 °C. Ar atmosphere with a gas flow of 20 ml/min was used. The sample powder of 30–40 mg, loaded in an alumina liner within the platinum pan, was subjected to a heating rate of 10 K/min.

A Calvet-type DSC calorimeter, model mHTC 96 (Setaram), was used for determination of heat capacity of the selected mixtures. Two distinct types of measurements were conducted: one in the low-temperature range, where no mass loss is observed, and the other at high temperatures. In the first measurement, a powdered sample of 200–300 mg was loaded in an alumina liner within a platinum crucible. In the second measurement, a specimen of 50–100 mg was loaded into a sealed platinum tube in a platinum sample holder. A heating rate of 4 K/min under He with a flow of 5 ml/min was applied. Temperature and enthalpy calibration for the first measurement type were performed using the pure metals In (156.6 °C), Sn (231.9 °C), Pb (327.5 °C), Zn (419.5 °C), Al (660.3 °C) and Ag (961.8 °C). For the second measurement type, calibration was done with the pure salts $BaCO_3$ (808.0 °C), Na_2SO_4 (241 °C and 884 °C), K_2SO_4 (584 °C and 1069 °C), MgF_2 (1263 °C). The average temperature deviations were ±2 °C and ±6 °C for the first and second measurement types, respectively. The three-step ratio method [29] with sapphire (α-Al_2O_3, NIST Standard Reference Material SRM720, purity 99.95 %, metal basis) [30] as a reference was applied for the determination of the heat capacity (C_p°, J•mol^{-1}•K^{-1}) according to the following equation:

$$C_{p(s)}^{\circ} = \frac{m_r}{m_s} \cdot \frac{DSC_s - DSC_b}{DSC_r - DSC_b} \cdot C_{p(r)}^{\circ} \quad (1)$$

where m is the mass of the substance (g), DSC is the signal of thermopile (μV), and subscripts b, r and s stand for baseline, reference and sample respectively. Baseline and reference measurements were performed for each measured sample separately. The sapphire reference used in the experiments varied based on the specific instrument and setup. For the Netzsch DSC, the sapphire reference was a disc-shaped specimen of mass comparable to that of the sample mass under analysis. For the Setaram DSC, two configurations were used depending on the crucible type. When a platinum crucible with an alumina liner was used, stacked sapphire discs were employed as reference. Alternatively, when platinum tubes were used as crucibles, small sapphire cylinders with a diameter of approximately 1 mm were used.

2.2.3. High Temperature X-Ray Diffractometry (HTXRD)

An Emperyean diffractometer from Malvern PANalytical equipped with a Cu-LFF X-ray tube (operated at 40 kV and 40 mA), BBHD mirror, a PIX-cel3D detector and a high temperature oven chamber Anton Paar HTK 1200 N was used for HTXRD analysis. A continuous flow of synthetic air was applied during the experiment. Lattice parameters and amounts of secondary phases were determined through Rietveld refinement using the profile analysis software TOPAS version 6 from Bruker AXS. Crystal structures were obtained from the Inorganic Crystal Structure Database (ICSD). The uncertainty for molar volume was estimated to be ±0.02 cm^3/mol and for temperature ±2 K. XRD investigation on $MgSO_4$:$CaSO_4$ mixtures was conducted on samples synthesised by solid-state reaction. The stoichiometric amount of anhydrous $MgSO_4$ and $CaSO_4$ were thoroughly mixed, grinded in an agate mortar and heated up to 900 °C for 72 h in a sealed quartz ampoule. During that time the heating was briefly interrupted (three times) to regrind the charges; the final powder was analysed by X-ray diffraction.

2.2.4. Microanalysis by Scanning Electron Microscopy (SEM) and Energy Dispersive X-ray spectroscopy (EDX)

Morphology and phase distribution were analysed by scanning electron microscopy using a Merlin (Zeiss Microscopy, Oberkochen, Germany) field emission scanning electron microscope (SEM) operated at 10 kV accelerating voltage and 0.5 nA probe current. Pellets of $CaSO_4$ and $MgSO_4$ were pressed and sintered for the EDX analysis. The non-conductive samples were sputter coated with Ir using a Q150T coater (Quorum Technologies, Laughton, UK) prior to SEM investigation. Images were acquired using an Everhart-Thornley secondary electron (SE) detector or a four-segment solid-state backscattered electron (BSE) detector. The local chemical composition was investigated by energy-dispersive X-ray (EDX) spectroscopy. Spectra were recorded using an X-max 80 silicon drift detector (Oxford Instruments, High Wycombe, UK). The AZtec software package (Oxford Instruments) was used for data acquisition and analysis. For the EDX analysis, areas were selected that were sufficiently large and had a flat surface. An accelerating voltage of 10 kV was used for the EDX analysis, so that the excitation volume is small compared to the grain size.

2.3. Self-referencing calibration method

In order to perform DSC measurements over a wide temperature range up to the melting of pure compounds and selected mixtures, experiments can be conducted using fully sealed crucibles in DSC Setaram mHTC 96. A customised platinum crucible, fabricated directly in the laboratory, was tested; the platinum tube was sealed by folding the ends into a book shape and flame-welding them. The sealed platinum tube containing the mixture under investigation was placed into a cylindrical

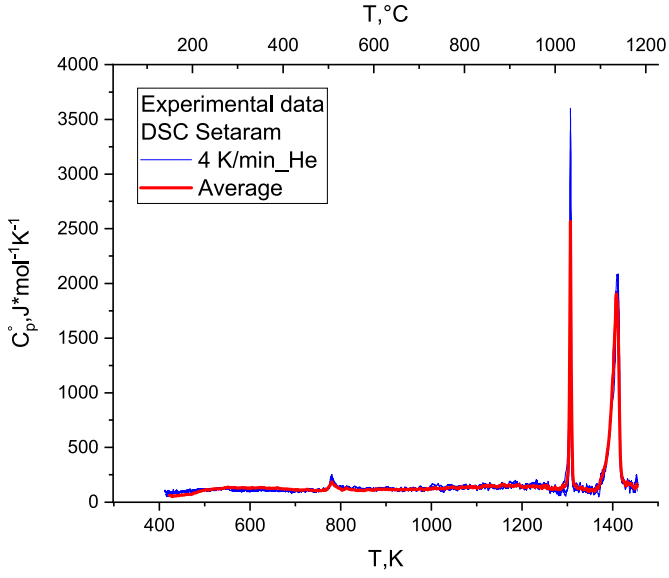

Fig. 1. Experimental values of molar heat capacity of $MgSO_4$ measured by DSC Setaram by applying SRCM method.

platinum sample holder (Fig. S 1) and loaded into the DSC device. It was observed that the three-step ratio method is influenced by different positioning and shape of the sealed platinum tube during baseline, reference and sample runs. Consequently, the resulting heat capacity curve displays an anomalous, but not uninformative trend.

Since the anomaly in the curve trends presumably arises from the purely practical handling cause, a novel method of correcting the experimental C_p curves is here proposed. This correction is based on reliable C_p curves obtained for the same compound in a temperature range below the decomposition temperature, where measurements were possible in open containers. If C_p curves in a stable temperature range can be accurately described by a polynomial function, it is expected that the experimental curve of the same sample over a wider temperature range will conform to the same polynomial trend [31]. This approach is referred to as a self-referencing calibration method SRCM. It consists of performing high temperature DSC measurements to obtain the initial experimental curve $C_{p,exp}$ using a sealed platinum tube in a platinum sample holder. A polynomial curve obtained from placing the sample in an Al_2O_3 liner in a platinum sample holder is utilised as the correction baseline $C_{p,correction}$ in order to determine the difference ΔC_p(T) between $C_{p,exp}$ and $C_{p,correction}$. The final curve $C_{p,corrected}$ is determined by applying the correction factor ΔC_p. This method has been validated using a well-known standard, confirming its reliability (Fig. S 2).

By applying the method proposed here, heat capacity curves can be obtained over a wide temperature range without any weight loss due to the decomposition of sulphates. Additionally, the method allows for the measurement of the C_p value of the liquid phase, which would otherwise be unattainable. While it is possible to integrate experimental C_p curves to derive enthalpy increment versus temperature curves, this approach is hindered by the anomalous trends of the experimental data, which do not yield the accurate vertical steps needed to calculate the enthalpies of transition. This limitation highlights the advantages of the proposed method. By performing a suitable calibration of standard salts in fully sealed platinum tubes, it becomes possible to derive the transition enthalpies from the areas subtended by the peaks and compare them with the relative values deduced from the enthalpy increment curves derived from the integration of $C_{p,corrected}$ curves.

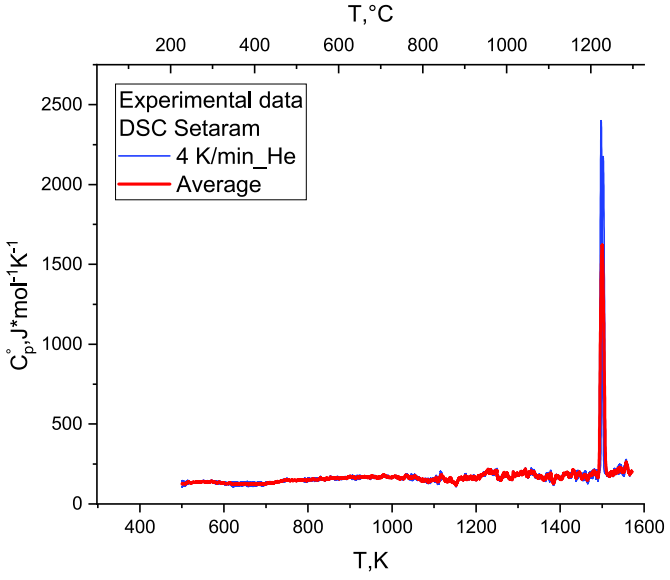

Fig. 2. Experimental values of molar heat capacity of $CaSO_4$ measured by DSC Setaram by applying SRCM method.

3. Thermodynamic modelling

3.1. Thermodynamic data of stochiometric compounds

Thermodynamic data (standard enthalpy of formation and standard entropy, $\Delta H^0_{298,f}$, S^0_{298}, and heat capacity as function of T, C_p(T), for pure solid and liquid compounds) are summarised in Table 1. Transition temperatures and heats of transformations (solid-solid, solid-liquid) are listed in Table 2. Thermodynamic data for $MgSO_4$ and $CaSO_4$ in the newly developed database were originally extracted from the SGPS database [32] and have been reassessed in Ref. [15], as well as in this study. The heat capacity C_p of stoichiometric compounds as function of temperature is described with power series in temperature [33], as shown in Equation (2).

$$C_p = A + B{\cdot}T + C{\cdot}T^{-2} + D{\cdot}T^2 + E{\cdot}T^3 + \ldots \quad (2)$$

In this work, the thermodynamic data of pure sulphates were updated based on the experimental data obtained, and the reassessment is presented in the corresponding sections below.

3.2. Thermodynamic model for liquid phase

The Gibbs energy of the liquid phase in the system was represented by the modified non-ideal associate species model proposed by Besmann et al. [34], which has proven applicability for complex oxide and salt liquids, e.g. in Refs. [14,35]. The sulphate liquid phase was considered as oxide solution to keep consistence with the general database [36]. The pure liquid sulphates were taken as solution components. The interactions between them are responsible for the thermodynamic properties of the liquid phase. To provide equal weighting of each associate species with regard to its entropic contribution in the ideal mixing term in the database, each species contains a total of two non-oxygen atoms per formula unit according to the model used in Besmann et al. [34]. This has been done to provide compatibility with the general oxide-salt database GTOx [36].

The molar Gibbs energy of the solution is presented by a three-term expression with contributions of the reference part, the ideal and the excess part considering binary interactions as follows:

$$G_m = \sum x_i {}^{\circ}G_i + RT\sum x_i \ln x_i + \sum\sum_{i<j} x_i x_j \sum_{\nu=0} L_{ij}^{(\nu)} (x_i - x_j)^{\nu} \quad (3)$$

where x_i is the mole fraction of phase constituent i (including the associate species), ${}^{\circ}G_i$ is the molar Gibbs energy of the pure (liquid) phase constituent i and $L_{ij}^{(\nu)}$ with $\nu = 0, 1, 2$ are the interaction coefficients between components i and j, according to the Redlich-Kister polynomial. ${}^{\circ}G_i$ and $L_{ij}^{(\nu)}$ are temperature dependent in the same way according to Equation (4):

$${}^{\circ}G_i, L_{ij}^{(\nu)} = A + BT + CT\ln(T) + DT^2 + ET^3 + F/T \quad (4)$$

Typically, in Equation (4), only the coefficients A and B are primarily considered and optimised.

3.3. Assessment of gibbs energy parameters

The assessment of the binary system presented in this study was performed, by combining the experimental data obtained from the present investigation with existing experimental information concerning phase diagram and thermodynamic properties. Firstly, the Gibbs energies of stoichiometric compounds were generated. The C_p functions of all substances were assessed before the optimisation and kept constant. Secondly, the binary interaction parameters ($L_{ij}^{(\nu)}$) between species ($MgSO_4$ and $CaSO_4$) in the liquid phase were optimised to obtain correct representation of phase equilibria. The optimisation of the selected

Table 1
Thermodynamic data of stochiometric compounds used in the present work.

Compound	$\Delta H^0_{298,f}$ J/mol	S^0_{298} J/mol•K	T K	C_p J/mol•K	Ref.
$MgSO_4$ (LT)	−1288800 [32]	91.6 [32]	1–42	$8.73213058\bullet10^{-5}T^3$	[15]
			42–298	$10.582036 + 0.44690916T + 34086.236T^{-2} - 4.7507286\bullet10^{-4}T^2 - 1740.55857/T$	[15]
			298–1283	$85.18297 + 0.08756883T - 1167240T^{-2} - 1.982192\bullet10^{-5}T^2$	[32]
			1283–2000	155	[32]
$MgSO_4$ (HT)	−1274200[a]	102.828[a]	LT→HT ΔH_{tr} = 14.6 kJ/mol at 1300.3 K (1027.1 °C), C_p like $MgSO_4$ (LT)		a
$MgSO_4$ (liquid)	−1238766[a]	120.880[a]	HT→L ΔH_{tr} = 43.4 kJ/mol at 1410.2 K (1137.0 °C)		[32], [a]
			1–42	$8.73213058\bullet10^{-5}T^3$	[15]
			42–298	$10.582036 + 0.44690916T + 34086.236T^{-2} - 4.7507286\bullet10^{-4}T^2 - 1740.55857/T$	[15]
			298–505	$85.18297 + 0.08756883T - 1167240T^{-2} - 1.982192\bullet10^{-5}T^2$	[32]
			505–2000	155	[32], [15]
$CaSO_4$ (LT)	−1437622 [32]	107.492 [39]	1–39	$1.58639676\bullet10^{-4}T^3$	[15]
			39–298	$60.2427676 + 0.22021804T + 73416.5259T^{-2} - 1.3048247\bullet10^{-4}T^2 - 4185.07635/T$	[15]
			298–1784	$100.854288 + 0.06896988T - 1736052.08T^{-2} - 8.6603105\bullet10^{-6}T^2$	[15]
			1784–2000	195.63	a
$CaSO_4$ (HT)	−1420012 [15]	119.282 [15]	LT→HT ΔH_{tr} = 17.6 kJ/mol at 1493.6 K (1220.4 °C), C_p like $CaSO_4$ (LT)		[15], a
$CaSO_4$ (liquid)	−1425938 [15]	107.714[a]	HT→L ΔH_m = 16 kJ/mol at 1783.6 K (1510.4 °C)		[15], a
			1–39	$1.58639676\bullet10^{-4}T^3$	[15]
			39–298	$60.2427676 + 0.22021804T + 73416.5259T^{-2} - 1.3048247\bullet10^{-4}T^2 - 4185.07635/T$	[15]
			298–795	$100.854288 + 0.06896988T - 1736052.08T^{-2} - 8.6603105\bullet10^{-6}T^2$	[15]
			795–2000	195.63	[15]
$CaMg(SO_4)_2$	−2678290[a]	249.173[a]	1–39	$2.459609818\bullet10^{-4}T^3$	a
			39–42	$60.2427676 + 0.22021804T + 73416.5259T^{-2} - 1.3048247\bullet10^{-4}T^2 - 4185.07635/T + 8.73213058\bullet10^{-5}T^3$	a
			42–298	$70.8248036 + 0.6671272T + 107502.76145T^{-2} - 6.0555533\bullet10^{-4}T^2 - 5925.63492/T$	a
			298–1800	$181.98396 + 0.17561T - 3004485.32926T^{-2} - 4.59679\bullet10^{-5}T^2$	a
$CaMg_2(SO_4)_3$	−4054080[a]	281.088[a]	1–39	$3.332822876\bullet10^{-4}T^3$	a
			39–42	$60.2427676 + 0.22021804T + 73416.5259T^{-2} - 1.3048247\bullet10^{-4}T^2 - 4185.07635/T + 1.746426116\bullet10^{-4}T^3$	a
			42–298	$81.4068396 + 1.11403636T + 141588.997T^{-2} - 1.08062819\bullet10^{-3}T^2 - 7666.19349/T$	a
			298–1800	$394.68198 - 0.01296T - 10918147.69689T^{-2} + 1.249221\bullet10^{-5}T^2$	a

[a] This work.

parameters based on the available experimental data (including own measurements) was performed using the CALPHAD Optimiser module included in the FactSage software [37,38].

4. Experimental results and discussion

4.1. $MgSO_4$

4.1.1. Transition temperatures

$MgSO_4$ exhibits thermal instability at around 1000 °C, decomposing prior to reaching its melting point [27,28]. As demonstrated by DTA/TG analysis conducted in open alumina crucible (Fig. S 3), the decomposition of $MgSO_4$ occurs at approximately 1000 °C, leading to the formation of magnesium oxide and sulphur oxides. A mass loss of 66.90 % demonstrates complete decomposition of sulphate to metal oxide. The DTA investigation in sealed platinum tubes enabled the identification of the transition temperatures by suppressing the decomposition reaction. The solid-solid transition was identified at 1028 °C (1301 K), and the solid-liquid transition at 1136 °C (1409 K). Phase transition temperatures of $MgSO_4$ obtained in the present work are compared with those found in literature in Table 2. The melting temperature detected by DTA analysis is in agreement with the value proposed by Rowe et al. [19] and adopted in the SGPS database [32]. The solid-solid transition temperature proposed in this study differs from the value of 1010 °C (1283 K) reported by Dewing and Richardson [40] and in use in SGPS database [32]. Based on the experimental findings of this work, the database is consequently updated. The transition temperatures were validated also by DSC measurements in sealed platinum tubes, giving values of 1030 °C (1303 K) and 1136 °C (1409 K).

4.1.2. Heat capacity and enthalpy increment

Due to the decomposition of $MgSO_4$ into MgO at temperatures above 1000 °C, DSC measurements in an open crucible are prevented over a wider temperature range up to the melting temperature. In the present study, DSC measurements in open platinum crucibles with alumina liner were conducted to obtain the heat capacity values and compare them with available literature data [41,49,50]. The heat capacity was measured in the temperature range 298–1050 K before decomposition takes place, using two different DSC devices described in section 2.2.2 with different heating rate (4 and 10 K/min). The mass loss after heating up to 1050 K was less than 0.5 %.

The self-referencing calibration method SRCM (section 2.3) allowed solving the decomposition problem and reaching the melting temperature of the sulphate. The final curves $C_{p,corrected}$ are shown in Fig. 1. The enthalpy of the solid-solid transition and of fusion are summarised in Table 2. The enthalpy of the solid-solid transition was determined to be 14.6 kJ/mol based on energy calibration, as described in section 2.2.2, and 14.7 kJ/mol from the integration of C_p curves. For the fusion enthalpy, values of 41.4 kJ/mol and 45.3 kJ/mol were obtained from calibration and integration, respectively. The enthalpy values are reported as the average of the two methods and provided as final experimental results: 14.6 ± 0.4 and 43.4 ± 2.0 kJ/mol. In contrast to the DSC curves recorded in open crucibles, an additional peak is evident at temperatures of around 780 K in the heating cycles, and absent during cooling. XRD investigations did not show any impurity in the $MgSO_4$ tested directly from the as-purchased chemical or after drying in a furnace at 150 °C. A plausible source of this effect could be a possible water content. Indeed, samples tested in open crucibles only showed that peak in the first heating curve. A further attempt at drying and

Table 2
Transition data of pure compounds.

Reaction	Reaction Type	Temperature of transition		Heat of transition	
		T_{tr}, °C (K)	Ref.	ΔH_{tr}, kJ/mol	Ref.
$MgSO_4$					
$MgSO_4$ (LT) ↔ $MgSO_4$ (HT)	solid↔solid	1010 (1373)	[40]		
		997-1095 (1270–1368)	[19]		
		1010 (1283)	[15, 32, 37]	3	[32, 37, 41]
		1027.1 (1300.3)	a		
		1029.9 (1303.1)	b	14.6	b
$MgSO_4$ (HT) ↔ liquid	melting	1124 (1397)	[27]		
		1120 (1393)	[28]		
		1185 (1458)	[42]		
		1136 (1409)	[19]		
		1137 (1410)	[15, 32, 41]	14.6	[15, 32]
		1137 (1410)	[37]	23.6	[37]
		1135.6 (1408.8)	a		
		1135.7 (1408.9)	b	43.4	b
$CaSO_4$					
$CaSO_4$ (LT) ↔ $CaSO_4$ (HT)	solid↔solid	1196 (1469)	[43]		
		1195 (1468)	[19, 26, 44]		
		1199 (1472)	[45]	29.43	[45]
		1211 (1484)	[46]		
		1201 (1474)	[47]	9.12	[47]
		1200 (1473)	[32, 37]	5	[32, 37]
		1227.4 (1500.6)	[15, 25]	17.61	[15, 25]
		1220.4 (1493.6)	a		
		1222.6 (1495.8)	b	17.7	b
$CaSO_4$ (HT) ↔ liquid	melting	1380 (1653)	[44]		
		1450 (1723)	[43]		
		1462 (1735)	[26]		
		1528 (1801)	[48]		
		1506.8 (1779.9)	[25]		
		1460 (1733)	[32]	25.4	[32]
		1527 (1800)	[37]	36.84	[37]
		1506.8 (1779.9)	[15, 25]	16	[15, 25]
		1510.4 (1783.6)	a		

[a] This work, DTA in sealed platinum tube.
[b] This work, DSC in sealed platinum tube.

removal of possible interference from the aqueous content was performed at 600 °C, but further DTA and DSC tests confirmed the presence of the peak, whose enthalpic contribution is considered negligible and therefore not included in the thermodynamic assessment.

4.2. $CaSO_4$

4.2.1. Transition temperatures

$CaSO_4$ decomposes into CaO above 1200 °C before reaching its melting temperature, making it difficult to measure the melting temperature, as discussed in Ref. [19]. DTA/TG investigations in open alumina crucibles recorded a mass loss of 60.85 % (Fig. S 4), equivalent to complete decomposition of sulphate to metal oxide. This phenomenon prevents the melting temperature to be reached, causing the pure compound to shift to a composition of the $CaSO_4$-CaO binary system. Therefore, the experimental values of the melting temperature [26] are to be considered as minimum values, less than or equal to the true melting temperature [19,48]. In the previous assessment [15], data on $CaSO_4$ were based on the experimental DTA measurement conducted by Kobertz and Müller [25]. The present work aimed to validate the transition temperatures by performing DTA and DSC investigations of $CaSO_4$ in sealed platinum tubes. The solid-solid transition was found to be at 1220 °C (1493 K) from DTA tests and 1223 °C (1496 K) from DSC analysis; with the melting occurring at 1510 °C (1783 K) from DTA investigation. The experimental values slightly differ from the previous DTA analysis [25], which reported transitions at 1227 °C (1550 K) and 1507 °C (1780 K).

4.2.2. Heat capacity and enthalpy increment

Three measurements were performed for each of the two DSC devices described in section 2.2.2, covering the temperature range 298–1350 K in alumina liners in platinum crucibles. They are consistent with data available in the literature [39].

Three measurements at high temperature in sealed platinum tubes in platinum crucibles were conducted using DSC Setaram (Fig. 2). According to the DSC Setaram settings using type B sample holder, the maximum measurable temperature was 1673 K (1400 °C). As a result, the melting temperature of the compound could not be reached during these measurements. Therefore, only the solid-solid transition enthalpy is proposed in this work. The experimentally determined values for the solid-solid transition enthalpy are 16.7 kJ/mol from calibration and 18.6 kJ/mol from integration. Considering the average value of 17.7 ± 1.0 kJ/mol, this result does not differ significantly from the value of 17.61 kJ/mol reported in the previous database [15], which was originally provided through DTA investigation [25]. Table 2 summarises the solid-solid transition enthalpy from this work and from other sources [32,37]. Given the validation of the value of the solid-solid transition enthalpy and the experimental impossibility of verifying the enthalpy of fusion, both previously proposed values are retained in the present work and in the related assessment of sulphate-containing systems. DTA tests, which reached temperatures up to 1600 °C, qualitatively confirmed the trend that the melting enthalpy is smaller than the solid-solid transition enthalpy (Fig. S 5). However, the enthalpy values derived from DTA are not considered fully reliable due to the inherent limitations of the technique, such as baseline shifts, heat flow inaccuracies, and the challenges of calibration at high temperatures in sealed platinum tubes. These factors can introduce significant uncertainties, making quantitative DTA-derived enthalpy values less dependable compared to those obtained from other methods like DSC.

4.3. $CaMg_2(SO_4)_3$

The calculated phase diagram [15,22], according to Rowe [19], suggests an intermediate compound with the stoichiometry $CaMg_3(SO_4)_4$. Smith et al. [23] clarified that the stoichiometry of the compound previously reported as $CaMg_3(SO_4)_4$ is not correct and density calculations showed it to be $CaMg_2(SO_4)_3$. Weil [51] presented the crystal structure of this double sulphate with lattice parameters: a = 8, 3072 Å, c = 7,3057 Å. V = 436,62 Å^3, hexagonal $P6_3/m$. In order to understand the composition of the intermediate compound, several experiments have been carried out by DTA and XRD. Several in-situ synthesised samples have been investigated, specifically with composition $CaSO_4$•$3MgSO_4$ and $CaSO_4$•$2MgSO_4$. High-temperature XRD tests on $CaSO_4$•$3MgSO_4$ revealed similar diffraction patterns to that of $CaMg_2(SO_4)_3$ across the sample (Fig. S 6). These findings suggest a high degree of structural similarity, leading to the conclusion that only one intermediate compound exists, corroborating the thesis of Smith et al. [23]. Despite the initial 1:3 composition, the sample showed two main phases: one consistent with $CaMg_2(SO_4)_3$ and the other with $CaSO_4$. The absence of detectable $MgSO_4$, which would be expected based on the

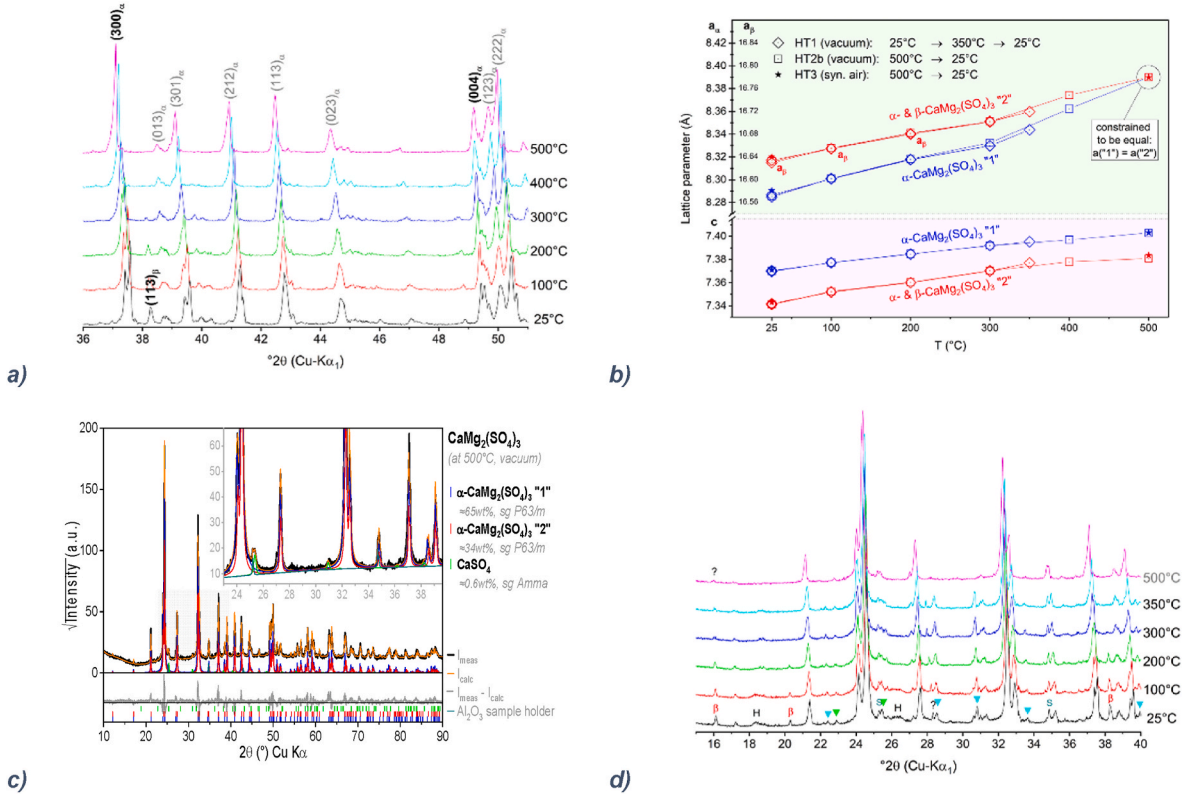

Fig. 3. ***a)*** *Visualisation of peak splitting due to lattice parameter differences of $CaMg_2(SO_4)_3$ phases;* ***b)*** *Temperature dependence of lattice parameters* a *(top) and* c *(bottom);* ***c)*** *HTXRD pattern of $CaMg_2(SO_4)_3$ at 500 °C under vacuum;* ***d)*** *Characteristic reflections: β = β-$CaMg_2(SO_4)_3$, ▼ = $CaSO_4$, ▼ = "unknown phase" (orthorhombic?), "H" = presumed hydrate phase, "?" = two additional not-identified phases, "S" = alumina sample holder (Intensity in square root scaling).*

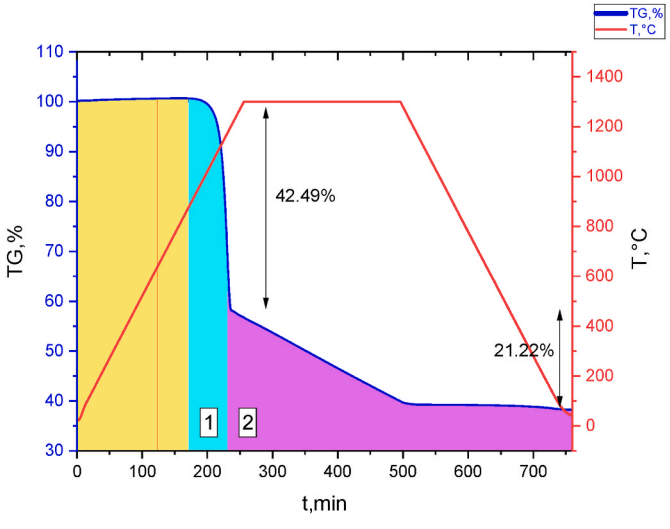

Fig. 4. TG curve of $CaMg_2(SO_4)_3$ in open alumina crucible.

starting composition, may be attributed to partial vaporisation of $MgSO_4$ or incomplete equilibration.

The sample $CaMg_2(SO_4)_3$ has been synthesised by solid state reaction, as described in section 2.2.3. Three experiments at high temperature were carried out in different atmosphere and reaching different temperatures: in vacuum ($P < 10^{-4}$ mbar) up to 350 °C; in vacuum ($P < 10^{-4}$ mbar) up to 500 °C; in synthetic air up to 500 °C. The targeted compound $CaMg_2(SO_4)_3$ tended to form multiple similar phases with slight differences in lattice parameters. Two hexagonal $CaMg_2(SO_4)_3$ polymorphs were found. One crystallizes in space group *P*63/m (176) with the following lattice parameters at room temperature: a ≈7.3 Å and c ≈ 8.3 Å [51]. This phase is named here as α-$CaMg_2(SO_4)_3$. The second polymorph (β-$CaMg_2(SO_4)_3$) crystallizes in space group P63 (173) with a c-lattice parameter similar to α-$CaMg_2(SO_4)_3$ but doubled a-lattice parameter [52]. Lattice parameters from the present work are listed in Table 3.

The thermal history seems to play an important role on the number of $CaMg_2(SO_4)_3$ phases formed as well as their crystallinity, as shown in Fig. 3. The diffraction patterns can be relatively well described by just two $CaMg_2(SO_4)_3$ phases, even if there are still some Bragg reflections not well fitted in the Rietveld refinement. At high temperatures (500 °C) their lattice parameters are almost identical, appearing almost as a single phase, even with the high-resolution setup of the diffractometer. At lower temperatures, the peak splitting due to lattice parameter differences becomes more obvious, as shown in Fig. 3a. Both polymorphs can be distinguished by the formation of additional superstructure reflections of β-$CaMg_2(SO_4)_3$ (the strongest at ca. 38.3°2θ, hkl: 113). The additional superstructure reflections of β-$CaMg_2(SO_4)_3$ were no longer detectable above 300 °C. At higher temperatures the diffraction patterns can be described by two α-$CaMg_2(SO_4)_3$ phases. Rietveld analyses indicates that only one (α-$CaMg_2(SO_4)_3$ "2") of the two phases transforms to β-$CaMg_2(SO_4)_3$. It might also be possible that, with increasing temperature, the relative intensities of the additional superstructure reflections are getting close to zero, because atoms are moving closer to special atomic positions of the crystal structure, like in α-$CaMg_2(SO_4)_3$. In this case no phase transition occurs and both structures α and β could not be distinguished at higher temperatures. The other phase (α-$CaMg_2(SO_4)_3$ "1") stays in α-$CaMg_2(SO_4)_3$ structure over the whole investigated temperature range. It seems that phase "2" has always a larger a-lattice parameter and a smaller c-lattice parameter than phase "1" (Fig. 3b). The sample contains approximately 1 wt% of $CaSO_4$. No changes in concentration were observed during the

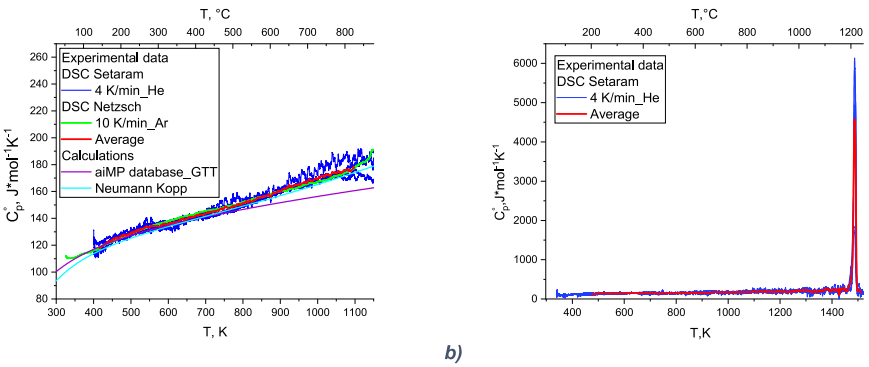

Fig. 5. Experimental values of molar heat capacity of $CaMg_2(SO_4)_3$ as $MgSO_4$(66.7 mol%)-$CaSO_4$(33.3 mol%): **a)** C_p of solid phase measured by two DSC devices and comparison with calculated values from databases [15,53]; **b)** C_p of solid and liquid phases measured by DSC Setaram by applying SRCM method.

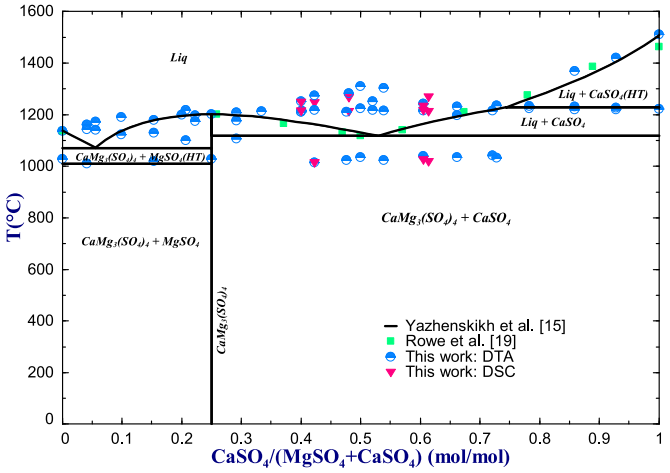

Fig. 6. Phase diagram of $MgSO_4$-$CaSO_4$, comparison of experimental data of this work with Rowe et al. [19] and Yazhenskikh et al. [15].

Table 3
Lattice parameters of $CaMg_2(SO_4)_3$.

T (°C)	phase	a (Å)	c (Å)	c/a	V (Å^3)
500	α-$CaMg_2(SO_4)_3$ "1"	8.390	7.403	0.882	451.3
	α-$CaMg_2(SO_4)_3$ "2"	8.390	7.381	0.880	449.9
25	α-$CaMg_2(SO_4)_3$ "1"	8.287	7.370	0.889	438.1
	β-$CaMg_2(SO_4)_3$ "2"	16.635	7.342		1758
	Recalculated for comparison	*8.317*	*7.342*	*0.883*	*439.6*

investigation. Reflections of an unknown phase were measured (marked in cyan in Fig. 3d). Attempts of indexing 9 characteristic reflections of the unknown phase suggested an orthorhombic base-centred symmetry. The phase vanishes on heating above 425 °C and reappears on cooling, as shown in Fig. 3d and in Fig. S 7.

4.3.1. *Transition temperature*

DTA investigation in open crucibles is hampered by decomposition of sulphate into oxides, as shown in Equation (5). $CaMg_2(SO_4)_3$ is stable up to 900 °C, as proved by DTA/TG measurements in open platinum tube. Above that temperature the system undergoes a mass loss of 62.44 %. The mass loss confirms the complete decomposition of the sulphate mixture 2:1 into metal oxides and sulphur dioxide (Equation (5)). According to the decomposition reaction, the residual mass fraction of metal oxides is 36.27 %.

$$CaMg_2(SO_4)_3(s,l) = CaO(s,l) + 2MgO(s,l) + 3SO_2(g) + 3/2O_2(g) \quad (5)$$

The decomposition of $CaMg_2(SO_4)_3$ proceeds through two distinct stages, as described in Equation (6) and illustrated in Fig. 4. In the first stage, occurring between 900 °C and 1100 °C, $CaMg_2(SO_4)_3$ partially decomposes to form magnesium oxide and calcium sulphate. This stage is characterised by an experimental mass loss of 42.17 %, which is in close agreement with the theoretical prediction of 42.49 %. The second stage, which takes place at temperatures above 1100 °C, involves further decomposition of the remaining compound $CaSO_4$, resulting in the formation of calcium oxide. This stage leads to an additional mass loss of 20.27 %, similar to the value of 21.22 % according to the second step of reaction. This means a cumulative mass loss of 62.44 %, consistent with the theoretical total decomposition value of 63.71 %. These results highlight the stepwise thermal decomposition behaviour of $CaMg_2(SO_4)_3$ and provide crucial insights for understanding its stability under high-temperature conditions.

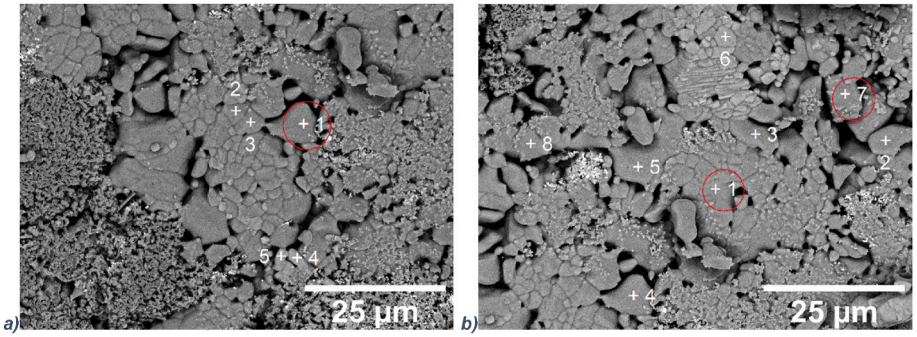

Fig. 7. SEM-Images (Back Scatter Electrons) showing the grains and phases of $MgSO_4$(70 mol%)-$CaSO_4$(30 mol%) across the sample surface, highlighting areas analysed by Energy Dispersive X-Ray Spectroscopy (EDX).

$$CaMg_2(SO_4)_3(s,l) \xrightarrow{1^{st}\,step} 2MgO(s,l) + CaSO_4(s,l) + 2SO_2(g) + O_2(g) \quad (6)$$

$$\xrightarrow{2^{nd}\,step} 2MgO(s,l) + CaO(s,l) + 3SO_2(g) + 3/2O_2(g)$$

DTA investigations were performed in sealed platinum tubes in a temperature range of 25–1300 °C. These analyses confirmed that the sample melts congruently at 1213 °C without undergoing any other phase transitions. Three separate samples were analysed in DTA using the mixture prepared by solid-state reaction. Other attempts were made to prepare the 2:1 mixture directly in platinum tubes for DTA analysis and then form the mixture in the first DTA heating-cooling cycle, in which case additional peaks are present as the mixture is not completely equilibrated, or at least slightly different in composition from the intermediate compound so that it is placed differently in the phase diagram. An internal validation of the melting temperature is offered by DSC measurements in sealed platinum tubes in DSC Setaram. Three measurements were performed giving a value of 1210 °C, in agreement with the value provided by the DTA analysis.

4.3.2. Heat capacity and enthalpy increment

The thermodynamic properties of the intermediate compound $CaMg_2(SO_4)_3$ have been investigated for the first time in the present work. Three measurements were performed with DSC (Netzsch) and three with DSC (Setaram) up to 1173 K (900 °C) with a final mass loss less than 1 wt%. The experiments were carried out in a platinum pan with alumina liner covered by a platinum lid. Fig. 5a shows the comparison of C_p obtained by DSC with Neumann-Kopp and ab-initio calculations (aiMP) [53]. The curves represent C_p of $CaMg_2(SO_4)_3$, considering its composition as $MgSO_4$(66.7 mol%)-$CaSO_4$(33.3 mol%), i.e., $Ca_{0.33}Mg_{0.67}SO_4$.

In order to cover a wider temperature range and to determine the enthalpy of fusion experimentally, the intermediate compound was analysed with DSC (Setaram) in sealed platinum tubes and the C_p curves corrected on the basis of the methodology presented earlier (Section 2.3), as shown in Fig. 5b. Three measurements were conducted for this purpose, which yielded an enthalpy of fusion value of 47.2 kJ/mol from calibration method and 49.7 kJ/mol from integration method, with an average value of 48.5 ± 1.3 kJ/mol, which was considered. The melting and crystallisation enthalpy values have good reproducibility, 47.4 and 47.0 kJ/mol, respectively, meeting one of the criteria for phase change materials. The experimental enthalpy of fusion of $CaMg_2(SO_4)_3$ is therefore 145.5 kJ/mol (Fig. S 8).

4.4. $MgSO_4$-$CaSO_4$ system

Experimental investigation of the $MgSO_4$-$CaSO_4$ system in open crucibles was hampered by the decomposition of both sulphates above 1000 °C [26–28]. Hence, it is needed to use closed containers to analyse such a sulphate system. Several crucible types, made from different materials (alumina, quartz and platinum) and with varying shapes, were tested to achieve temperatures of at least 1400 °C without any mass loss due to breakage or leakage (Fig. S 9). The most effective solution was found to be sealed platinum tubes (with diameter of 5 mm, thickness of 0.3 mm and length of 2–2.5 cm) containing the mixtures in their stoichiometric ratios. Attempting to prepare the mixtures by directly heating the two end-members in the DTA did not result in the desired

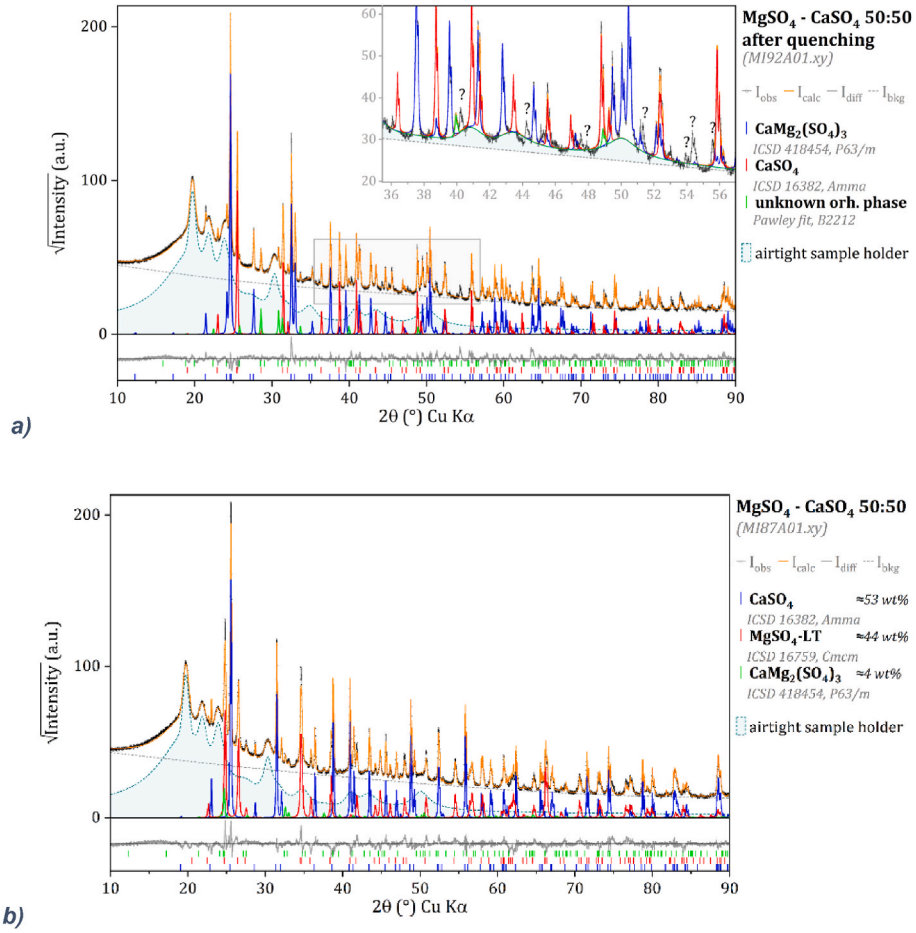

Fig. 8. XRD of $MgSO_4$-$CaSO_4$ with a stochiometric ratio of 1:1 **a)** sample subjected at heat treatment at 900 °C, followed by rapid cooling to room temperature; **b)** sample subjected at heat treatment at 900 °C, followed by controlled cooling at a rate of 5 K/min.

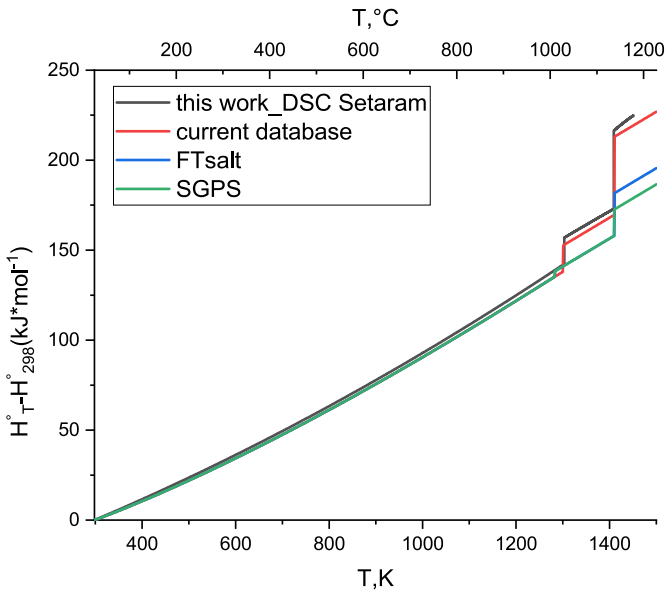

Fig. 9. Enthalpy increment of $MgSO_4$ obtained from DSC results in comparison with the current database and the commercial databases FTSalt [37] and SGPS [32].

formation of the target composition, and mass loss was observed. Generally, more reliable DTA investigations were conducted on mixtures that were pre-prepared by thoroughly mixing the end-members and annealing them at 1000–1100 °C for 48–72 h in quartz ampoules, followed by re-mixing and testing. Mixtures with a high content of $MgSO_4$ were found to be particularly susceptible to failure due to leakage at the crucible walls. Given the presence of the intermediate compound with congruent melting, a further attempt at thermal analysis of the binary system was performed by considering the aforementioned $MgSO_4$-$CaSO_4$ binary system into two sub-systems $MgSO_4$-$CaMg_2(SO_4)_3$ and $CaMg_2(SO_4)_3$-$CaSO_4$ by preparing the study mixtures by mixing $CaMg_2(SO_4)_3$ with either $MgSO_4$ or $CaSO_4$. This approach was driven by the need to form the compositions of interest and by the experimental evidence of the difficulty in preparing them directly from pure sulphates. Long-term annealing experiments were performed in order to equilibrate the mixtures. It has been demonstrated that compositions prepared by directly mixing pure sulphates have a far higher probability of failure, due to crucible compromise at high temperatures (above 1300 °C), compared to those prepared by mixing them with the intermediate compound. The reasons for this are not entirely understood, but probably the time and conditions to equilibrate the compositions of interest from pure sulphates make sample preparation more problematic, when compared to a mixture based on double sulphate precursors.

The experimental data points from DTA measurements of $MgSO_4$-$CaSO_4$ mixtures are summarised in Table S 1 and displayed in Fig. 6. The experimental data are compared with the phase diagram calculated using the previous assessment [15]. Unlike Rowe et al.'s data [19], in the present work the eutectic composition in the range near 50 mol% $CaSO_4$ was not identified; instead, additional thermal effects were detected. Examination of mixtures in this range produced experimental results that diverged significantly from previous values, suggesting alternative interpretations of the phase equilibria and indicating the potential presence of new phases. The DTA results of mixtures with compositions (47.63, 50.03, 53.85, 61.33, 72.10, 72.82 mol% $CaSO_4$) prepared by combining end-members revealed distinct thermal effects. Preliminary analysis raised the possibility that the mixtures had not fully equilibrated, as evidenced by the initial thermal effect observed at approximately 1020 °C. This thermal effect was thought to be associated with the solid-solid transition of residual pure $MgSO_4$ within the non-equilibrated mixture. Repeating the DTA measurements on identical mixtures and applying specific heat treatments to enhance equilibration yielded consistent results.

To validate this behaviour, the DTA thermal effects were indeed attributable to the tested compositions, similar tests were performed on mixtures in the same composition range, prepared by using the intermediate compound $CaMg_2(SO_4)_3$ and $CaSO_4$ as starting materials, thereby avoiding the presence of $MgSO_4$. These mixtures (42.21, 60.48, 66.10 mol% $CaSO_4$ in the system $MgSO_4$-$CaSO_4$, alternatively 36.54, 67.06, 74.36 mol% $CaSO_4$ in the system $CaMg_2(SO_4)_3$-$CaSO_4$) confirmed a consistent thermal effect at around 1020 °C, suggesting that the observed thermal event involved new phases rather than the solid-solid transition of $MgSO_4$.

To better understand the phase transitions of mixtures within the composition range of 40–75 mol% $CaSO_4$, and to address discrepancies with the data reported by Rowe et al. [19], samples in sealed platinum tubes were tested using a Setaram DSC. This approach aimed to validate the transition temperatures determined by DTA measurements and to provide more detailed results of their enthalpic contributions. The DSC analysis of samples (40.00, 42.21, 47.63, 48.02, 60.48, 61.33, 72.82 mol % $CaSO_4$) revealed a prominent peak between 1010 °C and 1030 °C in several cases, with an enthalpic contribution significantly higher than that of the second peak, which occurs at temperatures above 1200 °C (Fig. S 10). These findings suggest that the mixtures were indeed formed and equilibrated. If they had not, one would expect a low-temperature peak associated with the solid-solid transition of $MgSO_4$, which would be much less intense due to the minimal quantity of unreacted pure sulphate, and decrease further as the composition shifts towards the $CaSO_4$-rich side.

4.5. $CaMg(SO_4)_2$

The phase equilibria (Fig. 6) show a more complex behaviour than the initially assumed phase diagram and indicate the involvement of a previously unreported compound with a $MgSO_4$:$CaSO_4$ stoichiometry of 1:1, potentially accounting for the distinct thermal behaviour observed in the mixtures studied.

This hypothesis was further supported by Scanning Electron Microscopy (SEM) analysis of sulphate mixtures. Among the tested compositions, the specimen with 70 mol% $MgSO_4$ and 30 mol% $CaSO_4$ is presented here as a representative case, as it provided the clearest

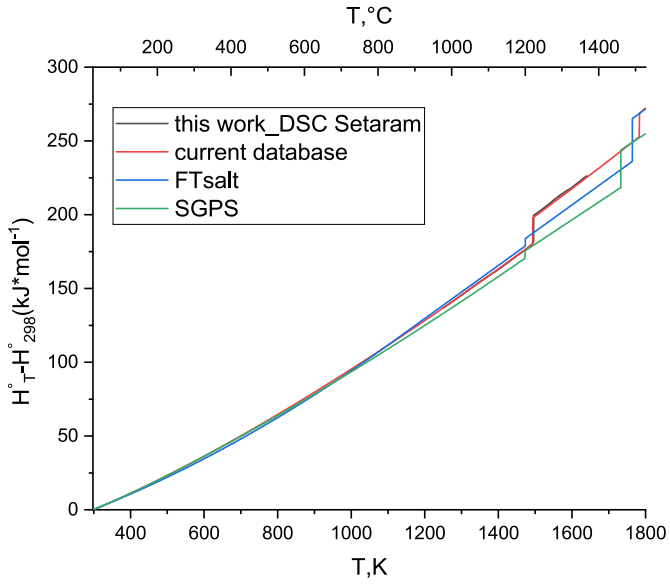

Fig. 10. Enthalpy increment of $CaSO_4$ obtained from DSC results in comparison with the current database and the commercial databases FTSalt [37] and SGPS [32].

microstructural evidence supporting the hypothesis. This choice is also related to the greater difficulty in pelletising sulphate mixtures with higher $CaSO_4$ content. The specimen with a composition of $MgSO_4$(70 mol%)-$CaSO_4$(30 mol%) was synthesised via a solid-state reaction. The synthesis involved a three-stage heat treatment (stage 1: 1050 °C for 72 h; stage 2: 950 °C for 45 h; stage 3: 1050 °C for 48 h), with intermittent grinding in an agate mortar. The mixture was then pelletised (100 mg, 5 mm diameter, 2 mm height) using a hydraulic press at 15 kN, followed by annealing under air at 600 °C for 24 h. Subsequent analysis confirmed the presence of phases with $MgSO_4$:$CaSO_4$ ratios of 1:1, 2:1, and 0:1, as shown in Fig. 7 and summarised in Table 4, all phases with medium-to-high $CaSO_4$ content despite the initial composition. This may indicate a more complex mechanism or incomplete reaction of the starting mixture. However, a detailed investigation of this behaviour lies beyond the scope of present work. Notably, this test reinforced the hypothesis of an intermediate 1:1 compound, first suggested by the DTA data, while also confirming the 2:1 compound discussed in detail in section 4.3 of this work.

A specimen with a $MgSO_4$:$CaSO_4$ ratio of 1:1 was synthesised by heating the mixture in a sealed quartz ampoule at 900 °C for 15 days, followed by rapid quenching to room temperature. XRD analysis revealed $CaMg_2(SO_4)_3$ as the primary phase and $CaSO_4$ as the second most abundant phase in a ratio of approximately 3:1. Additionally, an unknown orthorhombic phase was identified, accounting for 5–10 wt%, along with other minor unidentified secondary phases, as presented in Fig. 8a. While this orthorhombic phase could correspond to the hypothesised 1:1 compound, its detection - despite its minor abundance relative to the starting stoichiometry - confirms the existence of this compound. The limited quantity observed may be attributed to kinetic factors, such as incomplete reaction or sluggish nucleation and growth rates, which could hinder the full formation of the phase under the given experimental conditions. Additionally, the thermodynamic stability of the phase might be constrained to a narrow temperature or compositional window, resulting in preferential formation of competing phases.

To investigate further, a separate sample with the same 1:1 composition underwent heat treatment at 900 °C, followed by controlled cooling at a rate of 5 K/min. XRD analysis of this sample identified 53 wt % $CaSO_4$, 43 wt% $MgSO_4$ and 4 wt% $CaMg_2(SO_4)_3$, with no evidence of the orthorhombic phase, as illustrated in Fig. 8b. The variability in phase composition among the 1:1 samples subjected to different heat treatments, coupled with the SEM observations and DTA data, suggests the transient nature of the $MgSO_4$•$CaSO_4$ compound. This intermediate phase appears to be metastable, decomposing at lower temperatures into fine-grained exsolutions of $MgSO_4$ and $CaSO_4$, as evidenced by distinct microstructural features in the SEM images.

Further support for the existence of this 1:1 phase comes from the DTA analysis of an in-situ synthesised 1:1 mixture, which revealed three distinct thermal effects. The final thermal event corresponds to the congruent melting of the intermediate compound at approximately 1309 °C. This observation aligns with the hypothesis that the $CaMg(SO_4)_2$ phase exhibits stability only within a specific temperature range, existing as a distinct phase between approximately 1000 °C and its melting point. Beyond this range, it either decomposes or transforms into other phases, highlighting its limited thermal stability. In the phase diagram, the compound $CaMg(SO_4)_2$ is suggested to be stable from the low-temperature limit up to the congruent melting point. This transient behaviour underscores the intermediate nature of the compound, offering novel insights into the phase equilibria of the $MgSO_4$-$CaSO_4$ system.

Table 4
Molar percentages of elements detected in the analysed regions of the sample by SEM-EDX.

	Spectrum Label	O	Mg	S	Ca	Total (mol%)	$MgSO_4$: $CaSO_4$
Fig. 7a	Spectrum 1	67.7	8.3	17.7	6.3	100.0	1:1
	Spectrum 2	66.8	11.0	0.16.8	5.5	100.0	2:1
	Spectrum 3	66.6	11.2	16.6	5.6	100.0	2:1
	Spectrum 4	66.6	0.6	16.6	16.2	100.0	0:1
	Spectrum 5	66.9	0.6	15.6	15.6	100.0	0:1
Fig. 7b	Spectrum 1	68.3	6.3	18.3	7.1	100.0	1:1
	Spectrum 2	67.0	10.4	17.0	5.6	100.0	2:1
	Spectrum 3	66.7	10.8	16.7	5.8	100.0	2:1
	Spectrum 4	67.0	10.3	17.0	5.8	100.0	2:1
	Spectrum 5	66.8	10.6	16.8	5.8	100.0	2:1
	Spectrum 6	66.7	0.4	16.7	16.3	100.0	0:1
	Spectrum 7	67.8	7.4	17.8	7.0	100.0	1:1
	Spectrum 8	67.4	9.4	17.4	5.9	100.0	2:1

5. Thermodynamic assessment

5.1. $MgSO_4$

The low-temperature heat capacity based on [32,49] was previously assessed [15] and implemented in the database. For temperature above 505 K (Kauzmańs temperature), the C_p of the liquid phase was assumed to remain constant. The standard formation enthalpy and standard entropy were adopted from the SGPS database [32] and remained unchanged [15]. The thermodynamic properties of $MgSO_4$ are summarised in Table 1.

In the present work, it has been experimentally validated that the heat capacity can be described by the polynomial presented elsewhere [15]. The value of C_p of the liquid phase obtained experimentally by the SRCM method, and considered constant, is 154.5 J/(mol•K). This experimental value is in agreement with the value used in the current database of 155 J/(mol•K) [32,37], which, therefore, can be considered experimentally validated in the present work. Given the agreement of DSC measurements from the present work no C_p modifications have been included in the current database (Table 1).

In the previous work [15], the fusion enthalpy was adopted from the SGPS database [32] and Glushko's reference book [41]. From the DSC experiments, by appropriate sensitivity calibration or by integration of the C_p curves, the enthalpies of the phase transitions were calculated. The experimental transition enthalpies (solid-solid and melting) differ massively from the commercial databases [32,37]. Fig. 9 and Table 1 show the comparison of enthalpy data available in several thermodynamic databases with experimental results. On the basis of new experimental findings, the current database was updated in order to pursue the prediction of thermodynamic properties for systems involving $MgSO_4$. Thus, a value of 14.6 kJ/mol is proposed for the enthalpy of solid-solid transition and a value of 43.4 kJ/mol for the enthalpy of fusion. The phase transition temperatures were measured experimentally; the experimental melting temperature value conforms to those reported in the databases [32,37], and therefore no changes are made to the database in this work. However, the experimental evidence of the solid-solid transition temperature shows differences with the values reported elsewhere [32,37], and consequently a value of 1027.1 °C is entered into the database.

5.2. $CaSO_4$

This research builds upon the previous assessment [15], where new heat capacity polynomials were developed for the temperature range from 0 K to the melting point, based on experimental data [39]. The standard enthalpy and entropy values were sourced from the SGPS database [32] and Robie et al.'s work [39]. The C_p of the liquid phase was treated as constant above the temperature where the liquid and the solid entropies converge, and extrapolated below the melting point [15]. Experimental validation confirmed the values for heat capacity and solid-solid phase transition enthalpy (17.7 kJ/mol), resulting in no modifications to the database from the previous assessment. Therefore, enthalpy values of 17.6 and 16.0 kJ/mol obtained in Ref. [25] and used in the previous assessment [15] are considered for solid-solid and

solid-liquid phase transitions, respectively. The phase transition temperatures were measured experimentally, yielding new values that slightly differ from those previously reported in the literature [25,32,37]. These updated values, 1220 °C for the solid-solid transition and 1510 °C for melting, have been incorporated into the thermodynamic database.

5.3. $CaMg_2(SO_4)_3$

Experimental evidence on the existence of the intermediate compound $MgSO_4$:$CaSO_4$ with a stoichiometric ratio of 2:1 instead of 3:1 has led to the replacement of the pure compound in the current thermodynamic database. The initial values of standard formation enthalpy and standard entropy of the new compound were introduced based on the Neumann-Kopp rule, whereas heat capacity and solid-liquid transition enthalpy values were introduced according to experimental data. Fig. 5 presents a comparison of the C_p curves obtained in this study with those derived from the Neumann-Kopp rule and ab-initio calculations [54]. Fig. S 8 illustrates the comparison of enthalpy increments between experimental DSC measurements and those calculated using the current database. For the intermediate compound, the C_p of the solid phase has been described and introduced in the current thermodynamic database based on the experimental findings; the values of $\Delta H^0_{298,f}$ and S^0_{298} were optimised to describe the solid-liquid equilibria in the binary system (Table 1).

5.4. $CaMg(SO_4)_2$

Based on the experimental evidence presented in this study, the intermediate compound with a stoichiometric ratio of $MgSO_4$:$CaSO_4$ 1:1 was incorporated into the thermodynamic database to characterise the properties of the binary system. Initially, the enthalpy and entropy of formation $\Delta H^0_{298,f}$ and S^0_{298} for this intermediate compound were estimated using the Neumann-Kopp rule, based on the pure sulphate components. However, the experimental data detailed in section 4.5 indicate a potential thermal instability of the compound under investigation. To more accurately capture this behaviour, the enthalpy and entropy values initially assigned using the Neumann-Kopp approximation were subsequently optimised. The optimised values are summarised in Table 1. The optimisation was carried out to align the model more closely with the observed experimental results, thereby providing a more precise representation of the compound's thermal decomposition and stability limits within the binary system.

5.5. $MgSO_4$-$CaSO_4$ system

In the present work the re-assessment of the $MgSO_4$-$CaSO_4$ system was performed using the experimental phase diagram and calorimetric data from this study. The database was updated based on experimental evidence upon pure sulphates, and the new intermediate compounds 2:1 and 1:1.

The interaction parameters between $MgSO_4$ and $CaSO_4$ in the liquid phase were optimised using all phase equilibria and thermodynamic data from this work. The interaction parameters are listed in Table 5. The introduction of two intermediate compounds of different stoichiometry has considerably changed the liquidus curve of the phase diagram, compared with the previous assessment [15]. The phase diagram calculated using the new dataset is shown in Fig. 11. It shows overall good agreement with the experimental results, with some deviations observed in the $MgSO_4$-rich region. Nonetheless, the dataset is considered reliable, especially in view of the experimental challenges in assessing high-$MgSO_4$ compositions. The melting temperatures of the intermediate compounds, $CaMg_2(SO_4)_3$ and $CaMg(SO_4)_2$, were calculated at 1212.2 °C and 1313.3 °C, respectively. In addition, the eutectic point between $MgSO_4$ and $CaMg_2(SO_4)_3$ was predicted at 9.7 mol% $CaSO_4$ at 1089.2 °C. The eutectic between $CaMg_2(SO_4)_3$ and $CaMg(SO_4)_2$ was calculated to be very close to the congruent melting point of $CaMg(SO_4)_2$, 33.5 mol% $CaSO_4$ at 1213.0 °C. The calculated eutectic between $CaMg(SO_4)_2$ and $CaSO_4$ (71.5 mol% $CaSO_4$ at 1214.0 °C) was found in a good agreement with the data from Ref. [19] and the present measurements (71.5 mol% $CaSO_4$ at 1214.0 °C). While there is a slight disagreement with some phase diagram data points in the $MgSO_4$-rich composition region, this does not significantly affect the overall reliability of the dataset.

The calculated enthalpy of melting of the compound $CaMg_2(SO_4)_3$ (146.3 kJ/mol at 1212.2 °C) agrees very well with the measured values (145.5 kJ/mol at 1212.7 °C).

The optimised interaction parameters offer an enhanced thermodynamic dataset that closely aligns with the experimentally observed phase transitions, providing a more accurate representation of the system's phase behaviour.

Table 5
Thermodynamic descriptions of the liquid solution phases.

Gibbs energy data, J/mol	Ref.
$^\circ G_{MgSO_4} = {}^\circ G_{MgSO_4(liquid)}$	a
$^\circ G_{CaSO_4} = {}^\circ G_{CaSO_4(liquid)}$	[15]
$L^{(0)}_{CaSO_4,MgSO_4} = -10697.8 + 0.93{*}T$	a
$L^{(1)}_{CaSO_4,MgSO_4} = 5791.59 + 4.94{*}T$	a
$L^{(2)}_{CaSO_4,MgSO_4} = 2192.44$	a

[a] This work.

6. Conclusions

In this study, an experimental investigation of the $MgSO_4$-$CaSO_4$ binary system was conducted using thermal analysis techniques (DTA/TG and DSC) complemented by high-temperature X-ray diffraction (HTXRD) and scanning electron microscopy (SEM). A key achievement of this work was the successful synthesis and characterisation of an intermediate compound, $CaMg_2(SO_4)_3$. The thermodynamic properties of this compound, including its heat capacity, melting temperature (1213 °C) and latent heat of fusion (145.5 kJ/mol), were determined and reported for the first time. The solid-solid transition temperature of $MgSO_4$ was revised to 1027 °C, with updated transition enthalpies of 14.6 kJ/mol for the solid-solid transition and 43.4 kJ/mol for the solid-liquid transition. For $CaSO_4$, a solid-solid transition at 1220 °C and a melting temperature of 1510 °C were proposed. Additionally, the

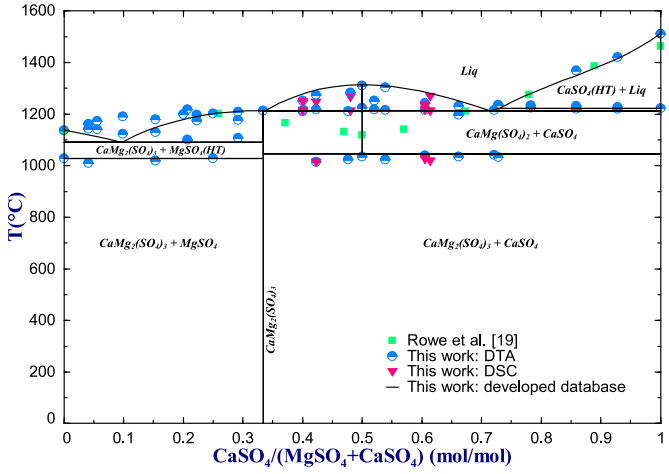

Fig. 11. Phase diagram of the $MgSO_4$-$CaSO_4$ system: comparison of experimental data of the present work with literature data [19] and the developed database.

intermediate compound $CaMg(SO_4)_2$, which exhibits thermal stability within a narrow temperature range, was identified. This compound has a congruent melting point at 1309 °C.

This study highlights the challenges in describing the phase equilibria of the compositions under investigation, particularly due to initial difficulties in equilibrating the mixtures and experimental evidence that diverges from previously reported literature. The thermodynamic dataset for the $MgSO_4$-$CaSO_4$ binary system was reassessed using the experimental data obtained in this study, including the Gibbs energy data on pure sulphates. That led to significant revisions in the thermodynamic properties of the system. Notably, the previously considered intermediate compound $CaMg_3(SO_4)_4$ was replaced by $CaMg_2(SO_4)_3$, and a new compound $CaMg(SO_4)_2$ was introduced, reflecting a more accurate description of the phase equilibria within the system.

This work provides a refined understanding of the $MgSO_4$-$CaSO_4$ binary system, offering new insights into its phase behaviour and thermodynamic properties, while also addressing discrepancies with earlier studies.

CRediT authorship contribution statement

Amedeo Morsa: Writing – review & editing, Writing – original draft, Visualization, Validation, Software, Methodology, Investigation, Formal analysis, Data curation, Conceptualization. **Elena Yazhenskikh:** Writing – review & editing, Validation, Software, Methodology, Data curation, Conceptualization. **Mirko Ziegner:** Validation, Methodology, Investigation. **Egbert Wessel:** Validation, Methodology, Investigation. **Rhys Dominic Jacob:** Writing – review & editing, Visualization, Data curation. **Michael Müller:** Writing – review & editing, Visualization, Validation, Supervision, Resources, Project administration, Methodology, Funding acquisition, Conceptualization. **Dmitry Sergeev:** Writing – review & editing, Visualization, Validation, Supervision, Project administration, Methodology, Funding acquisition, Conceptualization.

Declaration of competing interest

The authors declare that they have no known competing financial interests or personal relationships that could have appeared to influence the work reported in this paper.

Acknowledgements

This work was supported by the Federal Ministry for Economic Affairs and Climate Action on the basis of a decision by the German Bundestag within the project PCM-Screening 2 (FKZ 03EN6005D).

Appendix A. Supplementary data

Supplementary data to this article can be found online at https://doi.org/10.1016/j.calphad.2025.102855.

Data availability

Data will be made available on request.

References

[1] T. Kousksou, P. Bruel, A. Jamil, T. El Rhafiki, Y. Zeraouli, Energy storage: applications and challenges, Sol. Energy Mater. Sol. Cell. 120 (2014) 59–80.
[2] N. Eliaz, G. Shemesh, R. Latanision, Hot corrosion in gas turbine components, Eng. Fail. Anal. 9 (1) (2002) 31–43.
[3] N.S. Bornstein, Reviewing sulfidation corrosion—Yesterday and today, Jom 48 (1996) 37–39.
[4] C.C. Wang, K. Chen, T. Jiang, Y. Yang, Y. Song, H. Meng, B. Lin, Sulphur poisoning of solid oxide electrolysis cell anodes, Electrochim. Acta 269 (2018) 188–195.
[5] X. Luo, A. Wu, J. Sang, N. Huang, B. Han, C. Wang, Y. Gao, W. Guan, S.C. Singhal, The properties of the fuel electrode of solid oxide cells under simulated seawater electrolysis, Int. J. Hydrogen Energy 48 (28) (2023) 10359–10367.
[6] B. Cárdenas, N. León, High temperature latent heat thermal energy storage: phase change materials, design considerations and performance enhancement techniques, Renew. Sustain. Energy Rev. 27 (2013) 724–737.
[7] R. Jacob, M. Belusko, M. Liu, W. Saman, F. Bruno, Using renewables coupled with thermal energy storage to reduce natural gas consumption in higher temperature commercial/industrial applications, Renew. Energy 131 (2019) 1035–1046.
[8] M. Liu, W. Saman, F. Bruno, Review on storage materials and thermal performance enhancement techniques for high temperature phase change thermal storage systems, Renew. Sustain. Energy Rev. 16 (4) (2012) 2118–2132.
[9] P.D. Myers, D.Y. Goswami, Thermal energy storage using chloride salts and their eutectics, Appl. Therm. Eng. 109 (2016) 889–900.
[10] R. Jacob, M. Liu, Y. Sun, M. Belusko, F. Bruno, Characterisation of promising phase change materials for high temperature thermal energy storage, J. Energy Storage 24 (2019) 100801.
[11] Y. Wang, Y. Ma, Y. Lu, Q. Gao, Y. Wu, Y. Wang, C. Zhang, Phase diagram thermodynamic calculation of KNO3-NaNO2-KNO2 ternary system molten salt and its thermophysical properties investigation for thermal energy storage, J. Energy Storage 96 (2024) 112422.
[12] D. Sergeev, E. Yazhenskikh, D. Kobertz, K. Hack, M. Müller, Phase equilibria in the reciprocal NaCl–KCl–NaNO3–KNO3 system, Calphad 51 (2015) 111–124.
[13] D. Sergeev, B.H. Reis, I. Dreger, M.t. Baben, K. Hack, M. Müller, Thermodynamics of the Ca(NO3)2 – naNO3 system, Calphad 67 (2019).
[14] J. Qi, E. Yazhenskikh, M. Ziegner, X. Zhao, G. Wu, M. Müller, D. Sergeev, Experimental study and thermochemical assessment of the reciprocal system Li+, K +//Cl−, CO32, Calphad 83 (2023) 102603.
[15] E. Yazhenskikh, T. Jantzen, D. Kobertz, K. Hack, M. Müller, Critical thermodynamic evaluation of the binary sub-systems of the core sulphate system Na2SO4–K2SO4–MgSO4–CaSO4, Calphad 72 (2021).
[16] A. Hoshi, D.R. Mills, A. Bittar, T.S. Saitoh, Screening of high melting point phase change materials (PCM) in solar thermal concentrating technology based on CLFR, Sol. Energy 79 (3) (2005) 332–339.
[17] A. Abhat, Low temperature latent heat thermal energy storage: heat storage materials, Sol. Energy 30 (1983) 313–332.
[18] M.M. Kenisarin, High-temperature phase change materials for thermal energy storage, Renew. Sustain. Energy Rev. 14 (3) (2010) 955–970.
[19] J. Rowe, G. Morey, C. Silber, The ternary system K2SO4•MgSO4•CaSO4, J. Inorg. Nucl. Chem. 29 (1967) 925–942.
[20] L.S. Ramsdell, An X-ray study of the system K2SO4-MgSO4-CaSO4, Am. Mineral.: J. Earth Planet. Mater. 20 (8) (1935) 569–574.
[21] S.M. Mukimov, Z.I. Filippova, Reactions in melts of Na, K, Mg, and ca sulfates, Trudy Inst. Khim., Akad. Nauk Uzbek. SSSR, Inst. Khim 2 (1949) 123–132.
[22] H. Du, Thermodynamic assessment of the K2SO4-NaSO4-MgSO4-CaSO4 system, J. Phase Equil. 21 (2000) 6–18.
[23] D.H. Smith, M.R. Close, U. Grimm, Mg2Ca(SO4)3: correct stoichiometry of the coumpound previuosly reported as Mg3Ca(SO4)4, Energy Fuel. 10 (1996) 1241–1244.
[24] B.H. Reis, Development of a Novel Thermodynamic Database for Salt Systems with Potential as Phase Change Materials, BTU Cottbus-Senftenberg, 2021.
[25] D. Kobertz, M. Müller, Experimental studies and Re-assessment of the quasi-binary systems containing the sulfates of sodium, potassium, and calcium by differential thermal analysis and X-Ray diffraction in CALPHAD XL, CALPHAD XL (2011).
[26] J. Rowe, G. Morey, I. Hansen, The binary system K2SO4-CaSO4, J. Inorg. Nucl. Chem. 27 (1965) 53–58.
[27] R. Nacken, Ueber Langbeinit und Vanthoffit (K2SO4. 2MgSO4 und 3Na2SO4. MgSO4), Nachrichten von der Gesellschaft der Wissenschaften zu Göttingen, Mathematisch-Physikalische Klasse 1907 (1907) 602–613.
[28] A. Ginsberg, Über die Verbindungen von Magnesium-und Natriumsulfat, Z. Anorg. Chem. 61 (1) (1909) 122–136.
[29] A.S.f. Testing, Materials, Standard Test Method for Determining Specific Heat Capacity by Differential Scanning Calorimetry, ASTM International2011.
[30] D. Ditmars, S. Ishihara, S. Chang, G. Bernstein, E. West, Enthalpy and heat-capacity standard reference material: synthetic sapphire (α-Al2O3) from 10 to 2250 K, J. Res. Natl. Bur. Stand. 87 (2) (1982) 159.
[31] D. Sergeev, D. Kobertz, M. Müller, Thermodynamics of the NaCl–KCl system, Thermochim. Acta 606 (2015) 25–33.
[32] v13.1), SGPS - SGTE Pure Substances Database, 2019.
[33] K. Hack, The SGTE Casebook: Thermodynamics at Work, Elsevier2008.
[34] T.M. Besmann, K.E. Spear, Thermochemical modeling of oxide glasses, J. Am. Ceram. Soc. 85 (12) (2002) 2887–2894.
[35] E. Yazhenskikh, K. Hack, M. Müller, Critical thermodynamic evaluation of oxide systems relevant to fuel ashes and slags. Part 1: alkali oxide–silica systems, Calphad 30 (3) (2006) 270–276.
[36] Database GTOx, GTT-Technologies, Forschungszentrum Jülich, 2010-2020, GTT-technologies.
[37] C.W. Bale, E. Bélisle, P. Chartrand, S.A. Decterov, G. Eriksson, A.E. Gheribi, K. Hack, I.H. Jung, Y.B. Kang, J. Melançon, A.D. Pelton, S. Petersen, C. Robelin, J. Sangster, P. Spencer, M.A. Van Ende, FactSage thermochemical software and databases, 2010–2016, Calphad 54 (2016) 35–53.
[38] FactSage, Facility for the analysis of chemical thermodynamics, Version 8.3. Available from:: http://www.factsage.com/.
[39] R.A. Robie, S. Russell-Robinson, B.S. Hemingway, Heat capacities and entropies from 8 to 1000 K of langbeinite (K2Mg2 (SO4) 3), anhydrite (CaSO4) and of gypsum (CaSO4· 2H2O), Thermochim. Acta 139 (1989) 67–81.
[40] E. Dewing, F. Richardson, Decomposition equilibria for calcium and magnesium sulphates, Trans. Faraday Soc. 55 (1959) 611–615.

[41] V. Glushko, Termicheskie konstanty (thermal constants of substances), in: Online Reference Book, Moscow State University, Chemical Department, Moscow, 1982. http://www.chem.msu.ru/cgi-bin/tkv.pl?show=welcome.html.
[42] E. Jänecke, Über das Schmelz-und Erstarrungsbild des doppelt-ternären Systemes (K2· Na2· Mg)(Cl2· SO4), Z. Anorg. Chem. 261 (3-4) (1950) 213–225.
[43] W. Grahmann, Vergleich der Sulfate der Erdalkalien und des Bleis in den Temperatur-Konzentrationsdiagrammen mit Kaliumsulfat unter besonderer Berücksichtigung der Dimorphie von Anhydrit, Colestin, Baryt Und Anglesit, Voss1913.
[44] A. Bellanca, L'aftitalite nel sistema ternario K2SO4-Na2SO4-CaSO4, Period. Mineral. 13 (1942) 21–86.
[45] J. Torres, J. Mendez, M. Sukiennik, Transformation enthalpy of the alkali-earths sulfates (SrSO4, CaSO4, MgSO4, BaSO4), Thermochim. Acta 334 (1–2) (1999) 57–66.
[46] C. Pistorius, J. Boeyens, J. Clark, Phase diagrams of NaBF 4 and NaClO 4 to 40 kbar and the crystal-chemical relationship between structures of CaSO 4, AgMnO 4, BaSO 4 and high-NaClO 4, High. Temp. - High. Press. 1 (1969) 41–52.
[47] F. Tesfaye, D. Lindberg, L. Hupa, The K 2 SO 4–CaSO 4 system and its role in fouling and slagging during high-temperature processes. Materials Processing Fundamentals 2018, Springer, 2018, pp. 133–142.
[48] P. Coursol, A. Pelton, P. Chartrand, M. Zamalloa, The CaSO4-Na2SO4-CaO phase diagram, Can. Metall. Q. 44 (4) (2005) 537–546.
[49] G. Moore, K. Kelley, The specific heats at low temperatures of anhydrous sulfates of iron, magnesium, manganese, and potassium, J. Am. Chem. Soc. 64 (12) (1942) 2949–2951.
[50] K.K. Kelley, Contributions to the data on theoretical metallurgy, XIII. High-temperature heat-content, heat-capacity, and entropy data for the elements and inorganic compounds, in: Bulletin vol. 584, Bureau of Mines, 1960.
[51] M. Weil, Single crystal growth of CaMg2(SO4)3 via solid-/gas-phase reactions and its Nasicon-related crystal structure, Cryst. Res. Technol. 42 (11) (2007) 1058–1062.
[52] S.V. Krivovichev, E.P. Shcherbakova, T.P. Nishanbaev, The crystal structure of CaMg2(SO4)3, a mineral phase from coal dumps of the Chelyabinsk coal basin, Russia, Can. Mineral. 48 (6) (2011) 1469–1475.
[53] https://gtt-technologies.de/data/.
[54] v6.3, aiMP - Aioq Databases, 2024.